



RECENT RESEARCH ON LINK PERFORMANCE IN STEEL ECCENTRICALLY BRACED FRAMES

Taichiro OKAZAKI¹, Gabriela ARCE², Han-Choul RYU³, and Michael D. ENGELHARDT⁴

SUMMARY

A total of twenty-three tests were conducted to study the cyclic loading performance of links in seismic-resistant steel eccentrically braced frames (EBFs). Link specimens were constructed from five different wide-flange sections, all of ASTM A992 steel, with various lengths. These tests provided data on flange slenderness limits and overstrength factors for links, as well as on the effect of load history on link performance. A number of links tested in this program exhibited premature failure due to fracture of the link web at the termination of stiffener welds. This paper provides an overview of this experimental investigation, describing the overall research program, as well as details of the test specimens and key test results. The paper is concluded with a discussion of design implications for EBFs.

INTRODUCTION

The design intent for a steel Eccentrically Braced Frame (EBF) is that inelastic action under strong earthquake motion is restricted primarily to the links. The links, in turn, must be designed and detailed to provide large levels of cyclic ductility. The rather extensive experimental database on EBF link behavior, which has led to current building code rules, has been conducted almost exclusively on wide-flange shapes of ASTM A36 steel (Popov and Engelhardt [1]). However, in current practice, wide-flange sections are typically specified and supplied of the higher strength ASTM A992 steel. With the higher yield strength of 345 MPa for A992 steel, as opposed to 250 MPa of A36 steel, a number of rolled wide-flange shapes now violate flange slenderness limits in the *2002 AISC Seismic Provisions for Structural Steel Buildings* (AISC [2]), hereinafter referred to as the *2002 AISC Seismic Provisions*. Many of these same sections previously satisfied flange slenderness limits when made of A36 steel. The shift to A992 steel has therefore eliminated a number of rolled wide-flange shapes from use in EBFs. This, in turn, has led to questions on the appropriateness of current flange slenderness limits, particularly for shear yielding links. The effect of flange slenderness on link behavior has not been explicitly addressed in past research.

An additional issue of recent concern is the degree of overstrength that can be developed by a link. Link overstrength is defined as the maximum shear force developed by the link divided by the plastic shear strength of the link. Link overstrength is primarily due to strain hardening, but can also be due to the

1 Research Assistant, Dept. Civil Engineering, The University of Texas at Austin, Austin, Texas, USA.

2 Associate, CARBON Ingeniería S.A., San Jose, Costa Rica.

3 Research Assistant, Dept. Civil Engineering, The University of Texas at Austin, Austin, Texas, USA.

4 Professor, Dept. Civil Engineering, The University of Texas at Austin, Austin, Texas, USA

development of shear resistance in the link flanges. The link overstrength factor is used to estimate the maximum forces that can be generated by a fully yielded and strain hardened link, which in turn, is then used to design the diagonal brace, the beam segment outside of the link, and the columns of the EBF. Past researchers have generally recommended a link overstrength factor of 1.5 (Popov and Engelhardt [1]). Currently, the *2002 AISC Seismic Provisions* specify a link overstrength factor of 1.25 for design of the diagonal brace, and an overstrength factor of 1.1 for the design of the beam segment outside of the link and for the columns. As described in the Commentary of the *2002 AISC Seismic Provisions*, capacity design rules in the provisions are based on an assumed overstrength factor of 1.5. The actual specified factors are less than 1.5 for a number of reasons, including the use of the R_y factor to account for material overstrength, the use of resistance factors when computing the strength of the brace and other members outside of the link, the ability to sustain limited yielding in members outside of the link, and other factors. However, recent tests on large built-up shear links for use in bridge applications showed overstrength factors of nearly 2 (Itani *et al.* [3]; McDaniel *et al.* [4]). This has led to concerns that current overstrength factors may be unconservative, particularly for shapes with heavy flanges, where shear resistance of the flanges can contribute significantly to overstrength.

An experimental investigation was conducted to examine flange buckling and overstrength in links constructed of A992 steel. One objective of this investigation was to determine if the current flange slenderness limit can be relaxed to permit a larger number of rolled wide-flange shapes to be used as EBF links. The second objective was to reexamine link overstrength factors, particularly for rolled wide-flange shapes with a large ratio of flange to web area. A third objective of this experimental program was to evaluate the effect of loading sequence on link performance. The tests presented in this paper provide a sizable database on the behavior of EBF links constructed of A992 steel and detailed according to the *2002 AISC Seismic Provisions*. This experimental study was part of a larger investigation that included extensive analytical and finite element studies of EBF and link behavior. This paper only describes the experimental investigation. Information on the analytical and finite element studies is available in Richards and Uang [5, 6].

EXPERIMENTAL PROGRAM

Test Setup and Test Specimens

The test setup, shown in Fig. 1, was devised to reproduce the force and deformation environment imposed on a link in an EBF with one end of the link attached to a column. Each link specimen was welded to heavy end plates at each end, and these end plates were bolted into the test setup. The test setup was designed to accommodate a range of link sections and link lengths. Five different wide-flange shapes were used to construct the specimens, as listed in Table 1. All sections were of ASTM A992 steel. The actual measured yield and ultimate strength values are listed in Table 1 for samples taken from the edges of the flanges and from mid-depth of the web.

An objective of this research was to determine if the flange slenderness limit, $b_f/2t_f$, can be increased from the current limit of $0.30(E/F_y)^{1/2}$ to $0.38(E/F_y)^{1/2}$. The less stringent limit corresponds to that specified for plastic design in the *AISC Load and Resistance Factor Design Specification for Structural Steel Buildings* (AISC [7]). For $F_y = 345$ MPa (50 ksi), the current limit of $0.30(E/F_y)^{1/2}$ corresponds to 7.2, whereas the proposed new limit of $0.38(E/F_y)^{1/2}$ corresponds to 9.2. Table 1 lists the flange slenderness of the test sections. The W10x19, W10x68, and W18x40 sections satisfy the current flange slenderness limit of 7.2. The W16x36 and W10x33 sections were chosen because their flange slenderness violates the current limit, but is within the new proposed limit of 9.2. The W10x33 was chosen specifically because its flange slenderness is at the proposed new limit. Interestingly, the flange slenderness of the W16x36, based on the actual measured flange thickness and width, was substantially smaller than the nominal slenderness, and so the W16x36 test section actually satisfied the current limit of 7.2.

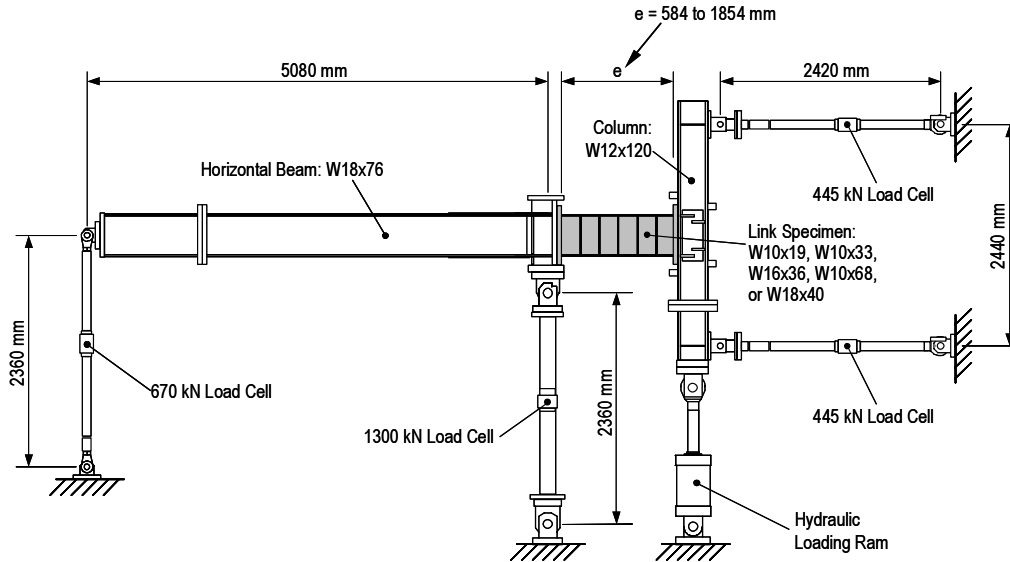


Fig. 1. Details of Test Setup

Table 1. Test Section Properties

Section	F_y (MPa)		F_u (MPa)		$b_f/2t_f$	
	Flange	Web	Flange	Web	Nominal	Actual
W10x19	367	405	509	531	5.1	5.2
W10x33	356	382	507	503	9.1	9.2
W16x36	362	392	534	565	8.1	7.1
W10x68	319	404	479	531	6.6	6.6
W18x40	352	393	499	527	5.7	6.1

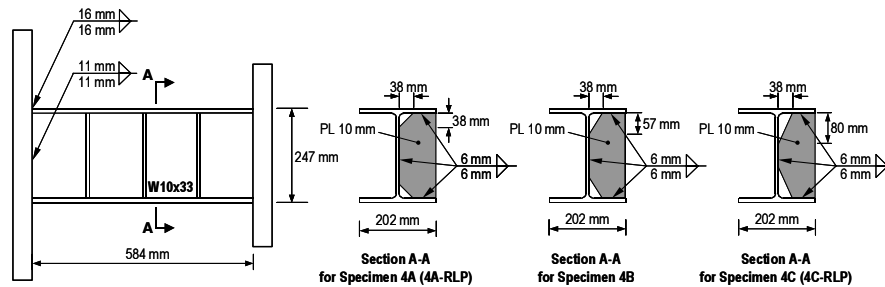
Note: The tabulated F_y is a static yield stress value, measured with the test machine cross-heads stationary. The tabulated F_u is a dynamic ultimate strength, measured with the test machine cross-heads in motion.

An additional objective of this project was to evaluate link overstrength, particularly for sections with large ratios of flange to web area. This was based on a concern that heavy flanges can contribute substantially to the shear capacity of the section, and therefore generate high levels of overstrength. In this test program, the W10x68 was chosen specifically to investigate this issue. The ratio of the area of one flange to the area of the web, for the W10x68, is approximately 2. This is near an upper bound of flange to web area for rolled wide-flange shapes likely to be used as links.

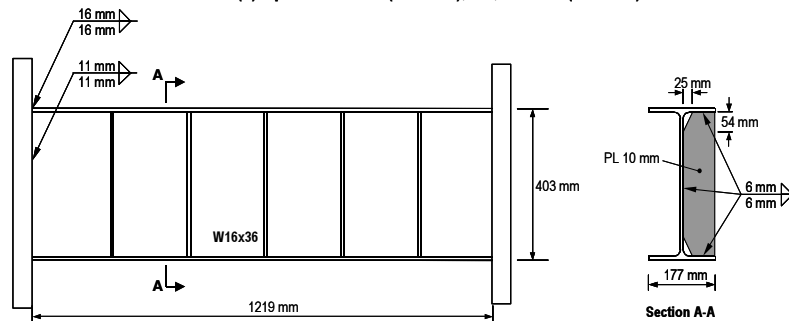
Table 2 provides a listing of all link test specimens. Fig. 2 shows schematic views of selected specimens. A range of link lengths were tested, ranging from very short shear yielding links to very long flexural yielding links. Links with a length less than $1.6M_p/V_p$ are dominated by shear yielding, whereas those longer than $2.6M_p/V_p$ are dominated by flexural yielding (AISC [2]). Between these limits, link inelastic response is heavily influenced both by shear and flexure. The link length parameter, $e/(M_p/V_p)$, listed in Table 2 was evaluated based on the measured section dimensions and the measured yield strength values. All link specimens were provided with intermediate stiffeners according to the 2002 AISC Seismic Provisions. The stiffener locations are listed in Table 2. As indicated in Fig. 2, stiffeners were provided

Table 2. Test Specimens

Specimen	Section	Link Length: e (mm)	$e/(M_p/V_p)$	Intermediate Stiffeners	Loading Protocol
1A	W10x19	584	1.73	3@ 146mm	AISC
1B	W10x19	584	1.73	3@ 146mm	AISC
1C	W10x19	584	1.73	3@ 146mm	AISC
2	W10x19	762	2.25	4@ 152mm	AISC
3	W10x19	1219	3.61	152mm from each end	AISC
4A	W10x33	584	1.04	3@ 146mm	AISC
4B	W10x33	584	1.04	3@ 146mm	AISC
4C	W10x33	584	1.04	3@ 146mm	AISC
5	W10x33	930	1.65	5@ 156mm	AISC
6A	W10x33	1219	2.16	4@ 244mm	AISC
6B	W10x33	1219	2.16	4@ 244mm	AISC
7	W10x33	1854	3.29	305mm from each end	AISC
8	W16x36	930	1.49	6@ 133mm	AISC
9	W16x36	1219	1.95	5@ 203mm	AISC
10	W10x68	930	1.25	2@ 305mm	AISC
11	W10x68	1219	1.64	3@ 305mm	AISC
12	W18x40	584	1.02	3@ 146mm	AISC
4A-RLP	W10x33	584	1.04	3@ 146mm	Revised
4C-RLP	W10x33	584	1.04	3@ 146mm	Revised
8-RLP	W16x36	930	1.49	6@ 133mm	Revised
10-RLP	W10x68	930	1.25	2@ 305mm	Revised
11-RLP	W10x68	1219	1.64	3@ 305mm	Revised
12-RLP	W18x40	584	1.02	3@ 146mm	Revised



(a) Specimens 4A (4A-RLP), 4B, and 4C (4C-RLP)



(b) Specimen 9

Fig. 2. Details of Selected Link Specimens

on only one side of the web, as permitted by the *2002 AISC Seismic Provisions* for link sections with a depth less than 635mm (25 in.). Stiffeners were full depth, welded to the web and both flanges using fillet welds.

Loading Protocol

Initially, seventeen tests were conducted using the loading protocol for EBF links specified in Appendix S of the *2002 AISC Seismic Provisions*. This protocol, hereafter referred to as the AISC protocol, requires applying increasing levels of cyclic link rotation angle, γ , which is computed as the relative displacement of one end of the link compared to the other, divided by the link length. After several initial elastic cycles, the protocol requires increasing the applied link rotation in increments of 0.01 rad, with two cycles of loading applied at each increment of rotation.

After observing a number of shear link specimens fail to achieve the link rotation required by the *2002 AISC Seismic Provisions*, it was decided that six of those specimens be duplicated and tested using a revised loading protocol recently developed and proposed by Richards and Uang [6]. The revised protocol was developed specifically for testing short shear links, based on extensive nonlinear time history analysis of EBFs. The revised protocol requires that, after completing the loading cycle at a link rotation of 0.05 rad, the link rotation be increased in increments of 0.02 rad, with one cycle of loading applied at each increment of rotation. The revised protocol is compared with the AISC protocol in Fig. 3.

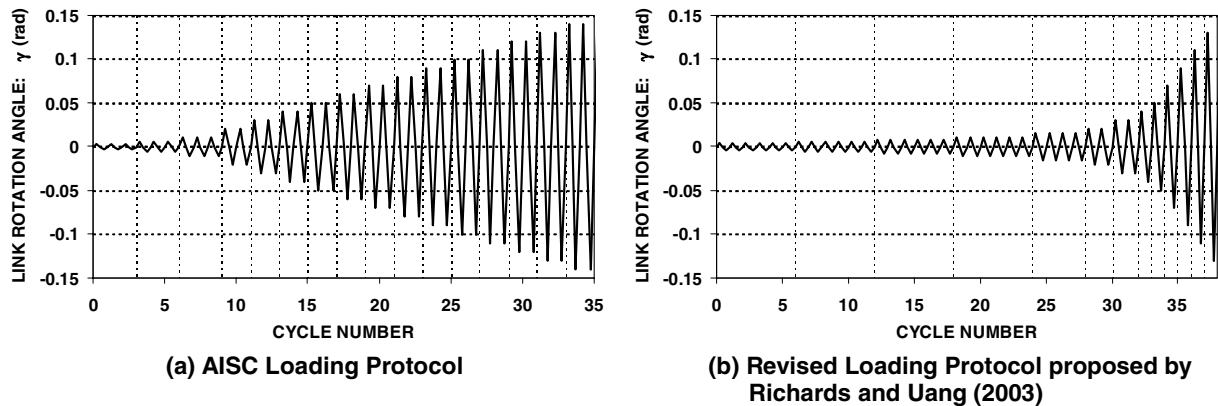


Fig. 3 Loading Protocols

TEST RESULTS

Acceptance criteria for links are defined in the *2002 AISC Seismic Provisions* based on inelastic rotation. The inelastic rotation, γ_p , is evaluated by removing the contributions of elastic response from the link rotation, γ . The provisions specify the shear yielding links ($e \leq 1.6M_p/V_p$) should be capable of developing an inelastic rotation of 0.08 rad, whereas flexural yielding links ($e \geq 2.6M_p/V_p$) should be capable of an inelastic rotation of 0.02 rad. The required inelastic rotation of intermediate length links ($1.6M_p/V_p < e < 2.6M_p/V_p$) is determined by linear interpolation between 0.08 and 0.02 rad. The inelastic rotation capacity of the link specimens was defined per the *2002 AISC Seismic Provisions*, as the maximum level of inelastic rotation sustained for at least one full cycle of loading prior to the link shear strength dropping below the nominal link shear strength.

Table 3 lists results for each of the link specimens tested in this program. The table lists the actual inelastic rotation achieved by each specimen, as well as the inelastic rotation required by the *2002 AISC Seismic Provisions*. Also listed is a brief description of the controlling failure mode for each specimen.

Table 3. Test Results

Spec.	γ_p (rad)		Observed failure mode
	Req'd	Test	
1A	0.072	0.040	Fracture at link end plate connection
1B	0.072	0.059	Fracture at link end plate connection
1C	0.072	0.079	Flange and web buckling followed by fracture in web
2	0.041	0.071	Flange and web buckling followed by fracture in flange near link end
3	0.020	0.039	Flange and web buckling followed by fracture in flange near link end
4A	0.080	0.060	Fracture of web at stiffener weld
4B	0.080	0.069	Fracture of web at stiffener weld
4C	0.080	0.079	Fracture of web at stiffener weld
5	0.077	0.066	Fracture of web at stiffener weld
6A	0.046	0.044	Fracture at link end plate connection
6B	0.046	0.057	Flange and web buckling followed by fracture in web
7	0.020	0.035	Flange, web, and lateral torsional buckling
8	0.080	0.078	Flange and web buckling followed by fracture in web at stiffener weld
9	0.059	0.047	Flange and web buckling
10	0.080	0.072	Fracture of web at stiffener weld
11	0.078	0.067	Fracture of web at stiffener weld
12	0.080	0.090	Fracture of web at stiffener weld accompanied by web buckling
4A-RLP	0.080	0.100	Fracture of web at stiffener weld
4C-RLP	0.080	0.119	Fracture of web at stiffener weld
8-RLP	0.080	0.117	Flange and web buckling followed by fracture in web at stiffener weld
10-RLP	0.080	0.113	Fracture of web at stiffener weld
11-RLP	0.078	0.081	Fracture of web at stiffener weld; link rotation limited by ram stroke
12-RLP	0.080	0.120	Fracture of web at stiffener weld accompanied by web buckling

Specimens 1A, 1B and 6A failed prematurely due to fractures at the fillet welds connecting the link flanges to the end plates. These failures are considered an artifact of the test setup, as the link end connections used for the specimens were not representative of typical link end connection details used in actual EBFs. Thus, while the failure of the end connections in these three specimens is of some interest, these three specimens will be excluded from the remaining discussion. Excluding Specimens 1A, 1B and 6A, there are twenty remaining specimens that were not affected by failures at the link end connections, and can therefore be considered as providing valid fundamental data on the behavior of links.

Table 3 indicates that eight specimens (besides Specimens 1A, 1B and 6A) failed to reach their link rotation requirements. These specimens were tested under the AISC loading protocol, and had a length in the range $1.0M_p/V_p < e < 2.0M_p/V_p$. Out of the eight specimens, all but one specimen experienced a common failure mode. The failure process initiated from fractures that formed at the vertical fillet welds connecting the link stiffeners to the link web. These fractures formed at the top and bottom termination points of the fillet welds, and often extended in the horizontal direction, parallel to the link flanges. Ultimately, rapid development of these cracks led to drastic reduction of the link shear resistance. Specimen 4A provides an example of a specimen that failed to meet the rotation requirement due to such failure. Fig. 4 shows the hysteretic response of this specimen and Fig. 5 shows the specimen after testing. Fractures running across the top and bottom of the web are visible in this photo. These fractures limited the inelastic rotation capacity of Specimen 4A to 0.06 rad, falling short of the 0.08 rad required by the *2002 AISC Seismic Provisions*. As shown in Fig. 4, the link web fracture ultimately induced abrupt and drastic strength degradation. The majority of shear link specimens tested using the AISC loading protocol failed to meet their inelastic rotation requirements due to this link web fracture. In fact, regardless of the loading protocol, all specimens with length of $e < 1.7M_p/V_p$ were controlled by this failure mode.

Specimen 9 was the only specimen that failed to meet the inelastic rotation requirement while not exhibiting the link web fracture. This specimen had an intermediate length link of $e = 2.0M_p/V_p$, and failed prematurely due to strength degradation associated with severe flange and web buckling near both link ends. Fig. 6 shows the hysteretic response of Specimen 9 and Fig. 6 shows the specimen after testing. Fig. 7 shows very significant concentration of deformation near both link ends, where the section was severely distorted due to combined flange and web buckling. Significant yielding is visible in the link web panels besides the end panels. The development of local buckling was associated with gradual strength degradation, as shown in Fig. 6.

Five specimens had longer links of the range $2.0M_p/V_p < e < 3.6M_p/V_p$. All five of these specimens successfully achieved their required link rotation, and ultimately failed due to combinations of severe flange buckling, web buckling, and in some cases, lateral torsional buckling. The link web fracture discussed above was not observed in these specimens. Specimen 7 provides an example of a specimen that significantly exceeded its inelastic rotation requirement, and ultimately failed due to inelastic instability induced by flexure. Fig. 8 shows the hysteretic response of this specimen and Fig. 9 shows one end of the specimen after testing. Extensive flange and web buckling is visible in the photo. Similar to

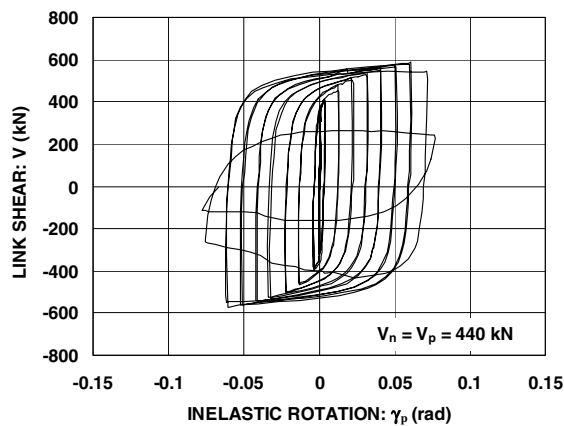


Fig. 4. Response of Specimen 4A

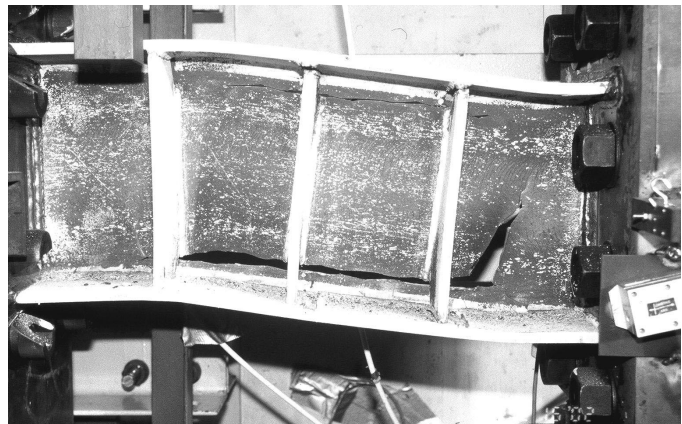


Fig. 5. Specimen 4A after testing

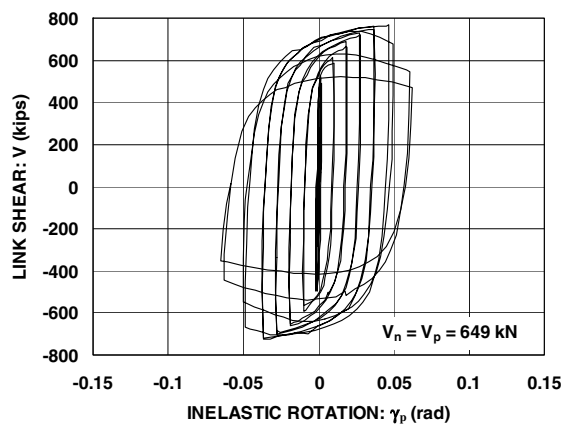


Fig. 6. Response of Specimen 9

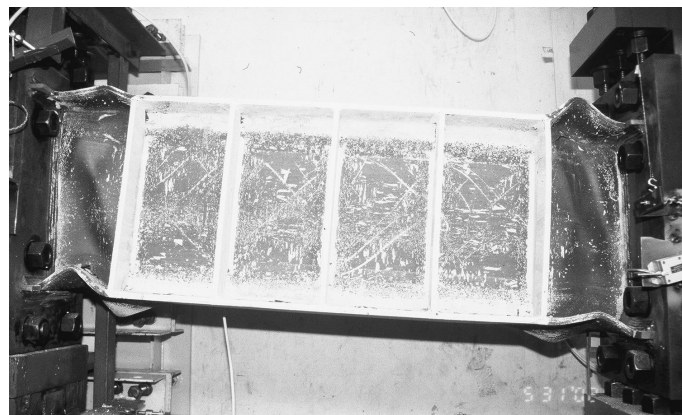


Fig. 7. Specimen 9 after testing

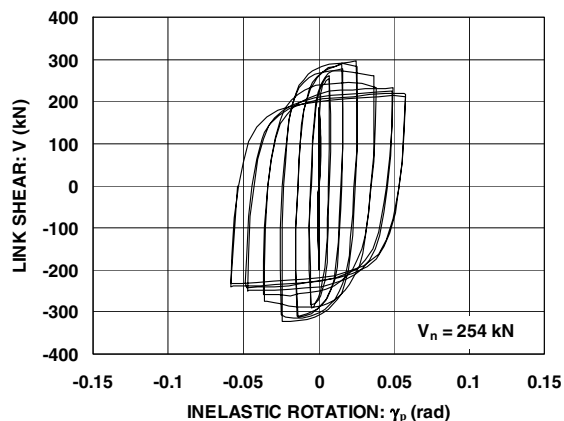


Fig. 8. Response of Specimen 7

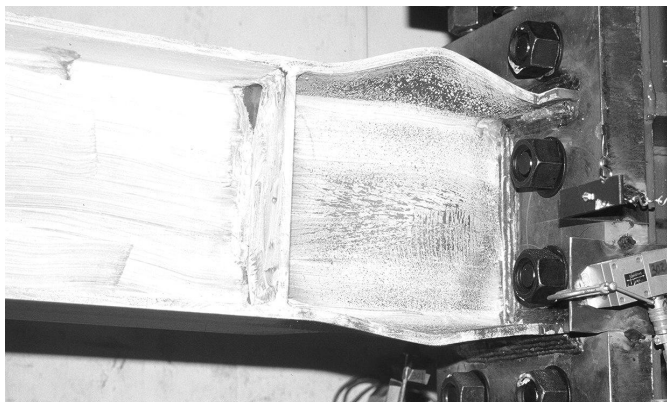


Fig. 9. Specimen 7 after testing

Specimen 9, the development of local buckling resulted in gradual strength degradation, as shown in Fig. 8. As illustrated by Specimen 7, the behavior of longer links ($2.0M_p/V_p < e < 3.6M_p/V_p$) was very similar to that reported in earlier tests, for example by Engelhardt and Popov [8].

DISCUSSION OF TEST RESULTS

Link Web Fracture

A notable feature observed in these tests, which was not typically reported in earlier tests, was fracture of web initiating at the stiffener welds. As discussed above, all specimens with links of $e < 1.7M_p/V_p$ failed due to the link web fracture. While fractures of link webs were reported in earlier tests, for example by Hjelmstad and Popov [9], and Malley and Popov [10], those fractures generally occurred after the development of severe web buckling. Fractures reported in earlier tests developed in link web panels at locations of large localized deformation due to local web or flange buckling, after inelastic instability caused significant degradation in link forces. Such fractures were also observed in this test program, for example in Specimens 1C and 6B, which achieved their required inelastic rotations under the AISC loading protocol.

Unlike the fractures reported in earlier tests, a number of specimens in this program developed web fractures at the ends of stiffener welds prior to the occurrence of any web buckling, or only after very mild buckling, as exhibited by Specimen 4A. This type of failure appears to be quite different from that observed in past tests. An exception is a recent test on a very large built-up link section tested for use in the new east span of the San Francisco-Oakland Bay Bridge (McDaniel *et al.* [4]). In this test, a fracture initiated at the termination of a stiffener weld prior to web buckling, although the fracture propagated diagonally across the web, compared to the horizontal fracture propagation observed in Specimen 4A. Analysis of the failure (McDaniel *et al.* [4]) suggested that the cause was a stress concentration at the end of the stiffener weld, because the stiffener was terminated too close to the flange-to-web groove weld of the built-up section. Based on finite element analysis, McDaniel *et al.* recommended terminating the stiffener weld farther from the flange-to-web weld, and suggested a minimum distance of three times the web thickness.

The first specimen in this program to exhibit a horizontal web fracture initiating at the end of a stiffener weld was Specimen 4A. After this failure, and based on the recommendations of McDaniel *et al.* [4], the stiffeners were terminated at a larger distance from the flange in the subsequent Specimens 4B and 4C. In going from Specimens 4A to 4B, and then to 4C, the termination of the stiffener weld was moved

progressively farther from the flange. In Specimen 4C, the stiffener welds were terminated a distance of approximately five times the web thickness from the “k-line” of the section (See Fig. 2a). The k-line is the location where the web meets the flange-web fillet. The test results (See Table 3) show that larger inelastic rotations were achieved, as the stiffener welds were moved farther from the k-line. However, even for Specimen 4C, which had the stiffener welds terminated quite a large distance from the k-line, the horizontal fractures still ultimately developed. Thus, while moving the stiffener welds farther from the k-line was beneficial, it did not eliminate the problem entirely. For all specimens tested after Specimens 4A to 4C, the stiffener welds were terminated a distance of five times the web thickness from the k-line, but many still exhibited fractures initiating at the stiffener ends.

Richards and Uang [5] noted three significant differences between the link specimens reported herein and those in earlier tests. These differences were: (a) stiffening criteria, (b) material, and (c) cyclic loading sequence. The influence of these three factors on the link web fracture is discussed in the following.

As noted by Richards and Uang [5], a large number of earlier link tests were conducted to investigate stiffener design criteria, and as such, the majority of these specimens did not satisfy current stiffener design criteria. The *2002 AISC Seismic Provisions* require tight stiffener spacing based on the realization that tighter spacing can control web buckling and result in superior cyclic ductility. As discussed above, the link web fracture observed in this program was not reported previously with the exception of McDaniel *et al.* [4], which also followed the current stiffener design criteria. Therefore, it is possible that the preclusion of web buckling shifts the critical failure mode to one controlled by fracture at the location of high constraints due to low cycle fatigue.

The proximity of the fractures in many of the test specimens to the k-line of the section suggests that material properties in the k-area may have played a role in these fractures. The *2002 AISC Seismic Provisions* indicate that the steel in the k-area of rolled wide-flange shapes (the region where the web meets the flange) can exhibit high hardness and be prone to fracture. Consequently, for the sections used in this test program, material properties were measured within this area. These measurements did in fact show highly elevated hardness levels and significantly reduced levels of tensile coupon elongation in the k-areas of the test sections, with the exception of the W10x19. Nonetheless, the role of the k-area material properties in the observed fractures is unclear.

After link web fracture was observed in a number of these test specimens, Richards and Uang [5] noted that the typical loading sequences used in shear link tests conducted in the 1970’s and 1980’s were less severe compared to the AISC protocol used for the tests in this current program. Further, there appeared to be no rational basis for the link loading protocol specified in Appendix S of the *2002 AISC Seismic Provisions*. As a result, Richards and Uang [6] developed a revised loading protocol for testing short shear links, which was used for the first time in this research. This revised loading protocol for shear links was developed using a methodology similar to that used for moment frame connection testing, as developed under the FEMA/SAC program (Krawinkler *et al.* [11]).

Six shear link specimens that experienced link web fracture in the initial series of tests in this program were duplicated and tested using the revised loading protocol. All six specimens, namely, 4A-RLP, 4C-RLP, 8-RLP, 10-RLP, 11-RLP and 12-RLP (RLP = Revised Loading Protocol) achieved link rotations well in excess of the required level. In fact, as indicated by the data in Table 3, these specimens developed inelastic rotations on the order of 25 to 50-percent greater than those required in the *2002 AISC Seismic Provisions*. It should be noted that the inelastic rotation developed by Specimen 11-RLP was limited due to limitations in the stroke of the loading ram. Nonetheless, even this specimen developed an inelastic rotation that exceeded the required value. These results largely resolved the concerns raised by the initial link tests using the AISC loading protocol that shear links may not be capable of achieving the required inelastic rotation of 0.08 rad.

Currently, the cause of the link web fractures, which were not observed in earlier tests, is unclear. Research is continued by the authors to better understand the differences between the current tests and earlier tests. Specifically, further tests are being conducted to investigate the influence of the k-area material property, stiffening details, and loading sequence on the occurrence of link web fracture.

Loading Protocol

This test program permitted a direct comparison of the performance of nominally identical link specimens tested using two different loading protocols: the AISC loading protocol (per Appendix S of the 2002 *AISC Seismic Provisions*) versus the revised loading protocol (per Richards and Uang [6]). To illustrate the effect of loading protocol, Fig. 4 shows the hysteretic response of Specimen 4A, which was tested using the AISC loading protocol. In comparison, Fig. 10 shows the hysteretic response of Specimen 4A-RLP, which was nominally identical to Specimen 4A, except that 4A-RLP was tested using the revised loading protocol. Specimen 4A-RLP developed an inelastic rotation capacity of 0.10 rad, as compared to 0.06 rad for Specimen 4A.

As illustrated by Specimens 4A and 4A-RLP, the loading protocol used to test the link specimens has a very large effect on the inelastic rotation capacity achieved by the link. Links tested with the revised loading protocol achieved inelastic rotations that were from 27-percent to 67-percent greater than links tested with the AISC loading protocol. The average increase in inelastic rotation using the revised loading protocol was 50-percent. Since the loading protocol has such a large effect on link test results, it is important that loading protocols be selected that realistically reflect link demands under actual earthquake loading, as represented by the work by Richards and Uang [6]. The revised loading protocol by Richards and Uang currently only applies to short shear yielding links with a length $e \leq 1.6M_p/V_p$. This work should be extended to also develop a rational loading protocol for longer links.

Whereas the loading protocol had a large effect on link inelastic rotation capacity, the loading protocol did not significantly change the controlling failure mode of the link. Links tested using the AISC loading protocol exhibited essentially the same failure mode as the nominally identical links tested using the revised loading protocol. Links that failed due to fracture of the link web under the AISC loading protocol still failed by fracture of the link web under the revised loading protocol. Figure 11 is a photo of

Specimen 4A-RLP after testing, showing the link web fractures that ultimately caused failure of this specimen. This failure mode is very similar to that observed in Specimen 4A (See Fig. 5). However,

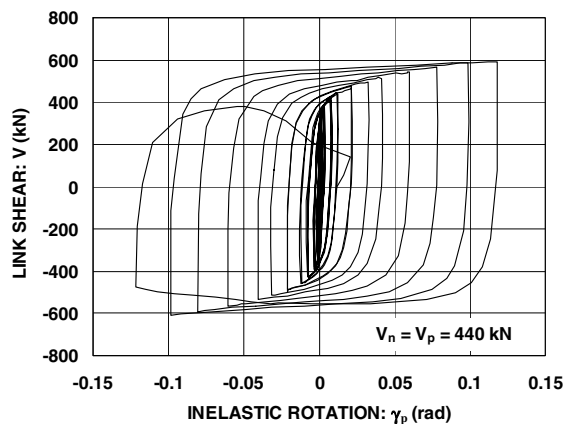


Fig. 10. Response of Specimen 4A-RLP



Fig. 11. Specimen 4A-RLP after testing

under the revised loading protocol, significantly higher inelastic rotations were achieved prior to link web fracture.

Regardless of loading protocol, many of the shear links tested in this research program failed by fracture of the link web initiating at the termination of stiffener welds. As described earlier, this failure mode was not typically observed in the extensive link testing programs conducted in the 1980s, which formed the basis for EBF detailing rules in the *AISC Seismic Provisions*. Consequently, links tested in this current program exhibited fundamentally different failure mechanisms than many links tested in earlier programs.

The results of the initial link tests using the AISC loading protocol indicated that link web fracture can be delayed by increasing the distance from the k-line to the termination of the stiffener to link web fillet weld. Results of tests using the revised loading protocol support this observation. Specimens 4A-RLP and 4C-RLP were both tested using the revised loading protocol. These specimens were identical except for the stiffener welding details. In Specimen 4A-RLP, the stiffener welds were terminated close to the k-line, whereas in Specimen 4C-RLP, the termination of the stiffener weld was moved farther from the k-line (See Fig. 2a). As indicated in Table 3, Specimen 4C-RLP achieved a greater inelastic rotation than Specimen 4A-RLP. (Specimen 4C-RLP achieved $\gamma_p = \pm 0.119$ radian; Specimen 4A-RLP achieved $\gamma_p = \pm 0.10$ radian). However, even with the stiffener weld terminated near the k-line, Specimen 4A-RLP still developed an inelastic rotation greater than the ± 0.08 radian required by the *2002 AISC Seismic Provisions*. Thus, providing a generous distance between the k-line and the stiffener weld termination, while perhaps not essential for satisfactory link performance, can result in higher link rotation capacity. In order to delay the onset of link web fracture, the stiffener welds were terminated a distance of $5*t_w$ from the k-line of the link section, where t_w is the link web thickness. Although chosen somewhat arbitrarily, this appears to provide a reasonable basis for design.

Flange Slenderness Ratio

A basic objective of this research program was to determine if the flange slenderness limit for links could be increased from the current limit of $0.30(E/F_y)^{1/2}$ to $0.38(E/F_y)^{1/2}$. In this test program, the flange slenderness of the W10x33 was very close to the proposed new limit of $0.38(E/F_y)^{1/2}$ for $F_y = 345$ MPa (50 ksi). Specimens with W10x33 sections were tested over a range of lengths varying from 1.0 to $3.6M_p/V_p$, covering a wide range of link behaviors from shear to flexural dominated response. The longer W10x33 specimens (Specimens 6B and 7) performed very well. These specimens exhibited severe flange buckling, but significantly exceeded their required rotation levels before link strength dropped below the defined failure threshold. The shorter W10x33 specimens tested using the AISC loading protocol (Specimens 4A to 4C and 5) did not achieve their required rotations due to premature web fractures, as discussed above. However, when retested using the more realistic revised loading protocol, short W10x33 specimens (Specimens 4A and 4C) significantly exceeded their required rotation levels. Therefore, data from the W10x33 test specimens support a relaxation in flange slenderness limits. Companion finite element simulations of EBF links by Richards and Uang [5], calibrated to the results of these tests, and extended to a wider range of link parameters, also support a relaxation in current flange slenderness limits.

The specimens constructed with W16x36 sections also provide useful data on flange slenderness effects. Based on nominal section dimensions, the flange slenderness of the W16x36 falls between the current limit of $0.30(E/F_y)^{1/2}$ and the proposed limit of $0.38(E/F_y)^{1/2}$. However, based on measured dimensions, the actual flange slenderness is smaller than the nominal value, and actually falls just within the current limit of $0.30(E/F_y)^{1/2}$. Of particular interest was Specimen 9, which was a W16x36 link with a length of $2.0M_p/V_p$. This specimen failed to achieve the required inelastic rotation angle due to strength degradation associated with severe combined flange and web buckling in the link end panels. This specimen experienced no fractures in the web, so strength degradation was entirely due to local buckling. The performance of this specimen suggests caution in relaxing flange slenderness limits for longer links.

The premature strength degradation in Specimen 9 appeared to result from interaction between flange and web buckling. The effect of flange-web interaction may be demonstrated by comparing Specimen 9 with Specimen 6B. The flange slenderness is smaller in Specimen 9, while the web slenderness, h/t_w , is smaller in Specimen 6B (measured $h/t_w = 53$ in Specimen 9; 31 in Specimen 6B). Both Specimens had an intermediate link ($e = 2.0M_p/V_p$ in Specimen 9; $2.2M_p/V_p$ in Specimen 6B). While both specimens ultimately failed due to strength degradation associated with flange and web buckling near both link ends, Specimen 6B achieved a larger inelastic rotation than Specimen 9 ($\gamma_p = 0.047$ in Specimen 9; 0.057 in Specimen 6B). Therefore, the specimen with a longer link, and hence a smaller required inelastic rotation, actually achieved a notably larger rotation. The link section that exhibited superior performance had larger flange slenderness but smaller web slenderness. Unlike Specimen 9, in which flange buckling appeared to be promoted by web buckling, local buckling in Specimen 6B was much more pronounced in the flanges than in the web. Therefore, flange-web interaction was much more substantial in Specimen 9. Although based on limited test data, the above comparison suggests that the web slenderness, in addition to flange slenderness, plays a critical role in the behavior of links. Meanwhile, finite element analysis by Richards and Uang [5] suggests that the current stiffening requirement for links of this immediate length range may not be adequate, and that Specimen 9 was significantly affected by this inappropriate stiffening. Richards and Uang recommend spacing stiffeners tighter near the ends for these links, since the combined flexure and shear generates a severe condition for local instability in those regions. Further research is warranted for the behavior of intermediate links in which severe interaction can occur between local flange and web buckling.

Based on the results of this testing program, combined with results from analytical studies (Richards and Uang [5]) and further combined with results from previous tests (Kasai and Popov [12]), there is strong and consistent evidence that the flange slenderness limit for shear yielding links ($e \leq 1.6M_p/V_p$) can be relaxed from the current limit of $0.30(E/F_y)^{1/2}$ to the proposed limit of $0.38(E/F_y)^{1/2}$. For longer links ($e > 1.6M_p/V_p$), the evidence on flange slenderness effects on link rotation capacity is not as clear. A number of longer link specimens with a flange slenderness at the proposed limit of $0.38(E/F_y)^{1/2}$ provided excellent performance, achieving inelastic rotations well beyond the required levels. However, a single specimen (Specimen 9) constructed with a W16x36 section failed to achieve the required inelastic rotation due to local buckling in the end panels. Consequently, further study is recommended prior to modifying the flange slenderness limit for link lengths greater than $1.6M_p/V_p$.

Link Overstrength

Data on overstrength for all specimens is presented in Table 4. For each specimen, this table lists the ratio V_{max}/V_n , where V_{max} is the largest shear force measured in a test. V_n is the inelastic strength of the link, and was calculated per the 2002 AISC Seismic Provisions as the smaller of V_p or $2M_p/e$, where V_p and M_p were computed using the actual measured dimensions and actual measured yield strengths of the test sections.

Table 4. Specimen Overstrength

Spec.	V_{max}/V_n	Spec.	V_{max}/V_n	Spec.	V_{max}/V_n
1A	1.20	5	1.34	12	1.40
1B	1.20	6A	1.21	4A-RLP	1.45
1C	1.23	6B	1.21	4C-RLP	1.48
2	1.24	7	1.28	8-RLP	1.37
3	1.25	8	1.35	10-RLP	1.47
4A	1.39	9	1.12	11-RLP	1.42
4B	1.42	10	1.44	12-RLP	1.44
4C	1.41	11	1.42		

The overstrength tended to be greater for shorter links, with lengths between 1.0 and $1.7M_p/V_p$, compared to longer links, with a length greater than $1.7M_p/V_p$. The average overstrength for these shorter link specimens was 1.42 , with a variation from 1.34 to 1.48 . That is, on average, the maximum shear force developed by these specimens was 1.42 times the link inelastic strength based on measured section and material properties. The average overstrength for the longer specimens ($e > 1.7M_p/V_p$) was 1.21 , with a variation from 1.12 to 1.28 .

The six specimens tested using the revised loading protocol exhibited a marginal increase in link overstrength compared to the corresponding specimens tested using the AISC loading protocol. This is believed to be due to the increased extent of strain hardening associated with the larger inelastic rotations.

Recent tests conducted by Itani *et al.* [3] and McDaniel *et al.* [4] exhibited significantly greater overstrength compared to earlier tests and the current tests. These tests differed from others in that the specimens were built-up links with a large section and different cross section proportions than rolled wide flange shapes typically used for EBFs. Further, these links were very short. Analysis by Richards and Uang [5] suggest these links experienced unusually high overstrength because of their very short length combined with the heavy flanges used in these built-up sections, which permitted the flanges to develop significant shear.

Specimens 10, 11, 10-RLP, and 11-RLP were made of the W10x68 section, which had a high ratio of flange to web area. Similar to the built-up sections discussed above, these four specimens were expected to develop large shear resistance in the flanges, and therefore, greater overstrength compared to the other specimens. However, the four specimens did not show unusually large values of link overstrength compared to other specimens in the same link length category. These results were confirmed by finite element simulations by Richards and Uang [5]. Therefore, the very large overstrength reported by Itani *et al.* [3] and McDaniel *et al.* [4] may not be a concern for links constructed of rolled shapes.

As described earlier, EBF design requirements in the *2002 AISC Seismic Provisions* are based on an assumed overstrength of 1.5 . The results summarized in Table 4 indicate that this assumed overstrength is reasonable, and perhaps somewhat conservative for longer links. However, for short links constructed of built-up shapes with heavy flanges, a higher overstrength factor, on the order of 1.75 to 2.0 , may be appropriate.

Specimen 9, which was intermediate length link of $e = 2M_p/V_p$, experienced a smaller overstrength compared to all other specimens. The smaller overstrength of links in this length range has been attributed to moment-shear interaction in strain-hardened intermediate length links (Engelhardt and Popov [8]).

CONCLUDING REMARKS

This paper presented data from a test program on the cyclic loading performance of EBF links made of ASTM A992 steel. The primary objectives of the test program were to reevaluate flange slenderness limits and overstrength factors for links.

Test data from this program indicate that the flange slenderness limit for shear yielding links ($e \leq 1.6M_p/V_p$) can be relaxed from the current limit of $0.30(E/F_y)^{1/2}$ to $0.38(E/F_y)^{1/2}$. This observation is supported by companion analytical studies and by results from previous tests. For longer links ($e > 1.6M_p/V_p$), the experimental evidence on flange slenderness effects is not as clear, and further investigation is needed before modifications to the flange slenderness limit can be recommended.

The ASTM A992 rolled W-shape links tested in this program exhibited overstrength factors ranging from 1.12 to 1.48 , with an overall average of 1.34 . When considering only shear yielding links, the average

overstrength factor was 1.42. Sections with high ratios of flange to web areas did not exhibit unusually high over-strength factors, at least within the range of flange to web area ratios typical of rolled W-shapes. The overstrength factor of 1.5, which forms the basis for EBF design requirements in the *2002 AISC Seismic Provisions*, appears reasonable for links constructed of typical rolled W-shapes. However, based on experimental and analytical results reported by others, for very short links constructed of built-up shapes with heavy flanges, a higher overstrength factor may be appropriate.

A number of shear link specimens tested in this program using the current AISC loading protocol failed to achieve required inelastic rotation levels due to fracture of the link web. These fractures initiated at terminations of stiffener to link web fillet welds. This type of fracture has not typically been observed in earlier link tests reported in the literature. Replicates of these specimens were retested using a recently developed revised loading protocol for shear links. All link specimens tested using the revised loading protocol achieved the inelastic rotations required in the *2002 AISC Seismic Provisions*. In fact, these specimens developed inelastic rotations on the order of 25 to 50-percent greater than those required in the *2002 AISC Seismic Provisions*.

Link web fracture can be delayed and link rotation capacity can be enhanced by increasing the distance from the k-line of the rolled link section to the termination of the stiffener to link web fillet weld. Based on the test results, it is recommended that stiffener welds be terminated a distance of at least $5t_w$ from the k-line of the link section, where t_w is the link web thickness.

Results of this test program clearly show that the loading protocol used to test EBF links has a very large effect on the inelastic rotation achieved by the links. Since the loading protocol has such a large effect on link test results, it is important that loading protocols be selected that realistically reflect link demands under actual earthquake loading, as represented by the revised loading protocol recently developed by Richards and Uang [6]. The revised loading protocol by Richards and Uang currently only applies to short shear yielding links with a length $e \leq 1.6M_p/V_p$. This work should be extended to also develop a rational loading protocol for longer links with a length greater than $1.6M_p/V_p$.

Research is continuing by the authors to further investigate the cause of link web fracture at the stiffener welds. Specifically, tests are being conducted to study the influence of the k-area material properties, stiffening details, and loading sequence on the occurrence of the link web fracture.

ACKNOWLEDGEMENTS

The writers gratefully acknowledge primary funding provided for this project by the American Institute of Steel Construction (AISC) and supplemental funding from the National Science Foundation (Grant No. CMS-0000031). The writers would like to particularly thank Tom Schlafly of AISC for his support and assistance throughout this project. The experimental work reported herein was conducted as part of a joint project with companion analytical studies at the University of California at San Diego (UCSD). The writers thank Prof. Chia-Ming Uang and Paul Richards at UCSD for their assistance, participation and collaboration in this project. The writers also thank James Malley, Subhash Goel and Tom Sabol for their assistance and advice on this project.

REFERENCES

1. Popov EP and Engelhardt MD. "Seismic eccentrically braced frames," *Journal of Constructional Steel Research*, 1988; 10: 321-354.
2. AISC. "Seismic provisions for structural steel buildings." Standard ANSI/AISC 341-02, American Institute of Steel Construction, Inc., Chicago, IL, 2002.

3. Itani A, Douglas BM, and El-Fass S. "Cyclic behavior of shear links in retrofitted Richmond-San Rafael Bridge towers." Proceedings of the First World Congress on Structural Engineering – San Francisco, Paper No. T155-3, Elsevier Science Ltd., 1998.
4. McDaniel CC, Uang C-M, and Seible F. "Cyclic testing of built-up steel shear links for the new bay bridge." Journal of Structural Engineering, American Society of Civil Engineers, 2003; 129(6): 801-809.
5. Richards P and Uang C-M. "Evaluation of Rotation Capacity and Overstrength of Links in Eccentrically Braced Frames (Phase 1)," Report No. SSRP-2002/18, Department of Structural Engineering, University of California at San Diego, La Jolla, CA, 2002.
6. Richards P and Uang C-M. "Development of testing protocol for short links in eccentrically braced frames," Report No. SSRP-2003/08, Department of Structural Engineering, University of California at San Diego, LaJolla, CA, 2003.
7. AISC. "Load and resistance factor design specification for structural steel buildings." American Institute of Steel Construction, Chicago, 1999.
8. Engelhardt MD and Popov EP. "Behavior of long links in eccentrically braced frames." Report No. UCB/EERC-89/01, Earthquake Engineering Research Center, University of California at Berkeley, Richmond, CA, 1989.
9. Hjelmstad KD and Popov EP. "Seismic behavior of active beam link in eccentrically braced frames." Report No. UCB/EERC-83/15, Earthquake Engineering Research Center, University of California at Berkeley, Richmond, CA, 1983.
10. Malley JO and Popov EP. "Design considerations for shear links in eccentrically braced frames." Report No. UCB/EERC-83/24, Earthquake Engineering Research Center, University of California at Berkeley, Richmond, CA, 1983.
11. Krawinkler H, Gupta A, Medina R, and Luco N. "Loading histories for seismic performance testing of SMRF components and assemblies," Report No. SAC/BD-00/10, SAC Joint Venture, 2000.
12. Kasai K and Popov EP. "A study of seismically resistant eccentrically braced frames." Report No. UCB/EERC-86/01, Earthquake Engineering Research Center, University of California at Berkeley, Richmond, CA, 1986.